



Microfibrillated celluloses produced from kraft pulp of coffee parchment

Marcela Ribeiro Coura¹ · Antonio Jacinto Demuner¹ · Robisnea Adriana Ribeiro² · Iara Fontes Demuner³ · Júlia de Cristo Figueiredo⁴ · Fernando José Borges Gomes⁴ · Verônica Oliveira de Paula Barbosa³ · Maria José Magalhães Firmino¹ · Ana Márcia Macedo Ladeira Carvalho³ · Daiane Einhardt Blank¹ · Marcelo Henrique dos Santos¹

Received: 26 April 2024 / Revised: 31 July 2024 / Accepted: 1 August 2024

© The Author(s), under exclusive licence to Springer-Verlag GmbH Germany, part of Springer Nature 2024

Abstract

The objective was to produce microfibrillated cellulose (MFC) and microfibrillated lignocellulose (MFLC) from waste materials, specifically coffee parchment. Additionally, the objective was to perform the characterization of the microcelluloses. Three MFCs were produced from kraft pulps (K#60, K#25, and Bleached), utilizing the conditions: pulp hydration and defibrillation using an ultra-refiner. The MFCs presented a chemical composition that is similar to the original pulps because they were produced through a purely mechanical process. It was obtained MFCs of highly viscous (5357 to 15,587 cP), even at very low consistencies (1.5%). The length of the samples ranged from 39 to 47 μm , and the measured diameters were 6820 nm (MFLC-K#60), 5600 nm (MFLC-K#25), and 5280 nm (MFC-Bleached). Due to these measurements, these materials were named microcelluloses. The crystallinity values were 52.5%, 58.8%, and 65.1% for the MFLC-K#60, MFLC-K#25, and MFC-Bleached samples, respectively. The thermogravimetric degradation curves were similar for the suspensions of MFC. The maximum degradation temperatures varied in the range of 322 to 339 °C. The infrared profiles of microfibrillated cellulose exhibited similar patterns, with distinct bands corresponding to the stretching and deformation of C-H, O-H, and C-O. The Zeta potential values obtained for MFLC-K#60, MFLC-K#25, and MFC-Bleached were -19.8 mV, -15.8 mV, and -27.4 mV, respectively. The water retention values for MFLC-K#60, MFLC-K#25, and MFC-Bleached were 792, 849, and 1032%, respectively. The pulp fibers from the parchment proved to be a viable alternative for the production of MFLC and MFC, as they presented comparable properties to microcellulose produced from wood.

Keywords Biomass · Mechanical defibrillation · Microcellulose · Coffee residue

1 Introduction

The growing demand for sustainability has encouraged the development and research of materials produced from renewable and sustainable sources. The primary objective is

to reduce the environmental impact associated with the disposal of petrochemical polymers [1–5]. In this context, biomass stands out as the most appealing raw material, given its status as the largest renewable resource on the planet [4, 6].

Lignocellulosic materials are predominantly composed of carbohydrates (cellulose and hemicelluloses) and lignin. Various sources of lignocellulosic materials can be found around the world. However, utilizing agro-industrial residues as a source of lignocellulosic biomass can help reduce the use of forest resources. This is particularly beneficial for regions with limited wood production, as it allows them to produce alternative pulps [1]. Therefore, it is important to emphasize the significance of studying alternative materials to wood in order to develop new biodegradable products.

Coffee is an important agricultural product, and it is estimated that 170.83 million bags (60 kg each) of coffee were

✉ Iara Fontes Demuner
iara.demuner@ufv.br

¹ Chemistry Department, Federal University of Viçosa, Viçosa, MG, Brazil

² SENAI Innovation Institute for Biosynthetics and Fibers, SENAI CETIQT, Rio de Janeiro, Brazil

³ Department of Forest Engineering, Federal University of Viçosa, Viçosa, MG, Brazil

⁴ Department of Forest Products, Federal Rural University of Rio de Janeiro, Seropédica, RJ, Brazil

produced globally in 2022/23 [7]. Brazil, in particular, has a robust coffee industry thanks to favorable conditions for coffee cultivation and advanced agricultural technology and infrastructure. In the country, the sector's compound annual growth rate (CAGR) is projected to reach 3.51% from 2023 to 2025, indicating a positive and steady market outlook [8].

During the processing of coffee beans, more than half of the fruit is discarded, which generates considerable waste [9]. Finding applications for this residue is attractive, as it is possible to add market value to by-products that were previously discarded and had caused environmental problems [6, 10]. Recent studies have revealed the potential for valorizing coffee waste.

In fact, Reichembach et al. [11] conducted a study on coffee wastes for the development of pectin-chitosan films. Laili et al. [12] explored coffee waste management and the possibility of creating a coffee-based eco-industrial park. Kim et al. [13] investigated the conversion of waste coffee grounds into microporous carbon materials, which showed excellent CO₂ capture performance and other benefits such as eco-friendliness, energy efficiency, and scalability. Král et al. [14] highlighted the bioactive compounds found in coffee husk and pulp, which have various applications such as food pigments, gelling agents, stabilizers, and extracts for enzyme production. Besides that, coffee by-products showed antimicrobial and antioxidant properties of phytochemicals [14, 15].

Coffee, cotton linter, bagasse, rice husk, and wheat straw generate different agricultural waste during their processing, rich in cellulose [4, 5, 16]. Cellulose is a biopolymer made up of anhydroglycopyranose units connected through β -1,4-glycosidic bonds. As the main component in the cell wall of plants, cellulose has the advantage of being renewable, biodegradable, and chemically versatile [1, 17].

Cellulose chains are joined by intra- and intermolecular hydrogen bonds and van der Waals forces between adjacent hydroxyl groups to form elementary fibrils. The elementary fibrils are held together to form microfibrils, with diameters ranging from 5 to 50 nm and lengths of several micrometers [18]. Cellulose fibrils are surrounded by lignin and hemicelluloses [19], forming a three-dimensional structure of the cell wall present in lignocellulosic biomass [1].

Natural polymers produced from renewable resources, including cellulose, are presently being used as an alternative to plastics due to their biodegradability, benign properties, widespread availability, and biocompatibility [20]. Cellulose obtained from different raw materials has diverse applications. Madivoli et al. [21] developed stimuli-responsive cellulose films for the detection of dimethyl amines. Joyline et al. [22] produced carboxymethyl cellulose from coconut fibers, which can be used to produce emulsifiers and superabsorbent polymers. Madivoli [23] demonstrated the potential of using natural polysaccharide, such as cellulose, in various

applications including wound dressings, tissue engineering, smart delivery vehicles for pesticides, fertilizers, therapeutic drugs, peptides, and proteins. Devarajan et al. [24] produced a hybrid AgNPs-TEMPO-mediated oxidation cellulose composite from jackfruit peduncle agro-waste, which can be applied in electronic devices.

In recent years, with the concept of biorefinery, interest in cellulose-based nanoparticles has been growing. These materials are biocompatible and feature excellent chemical, mechanical, and optical properties. In addition, they are highly reactive due to the hydroxyl groups present on their surface. Thus, micro- and nanocelluloses are highly attractive biopolymers for several applications [25–28].

Micro- and nanocelluloses are produced through the processing of lignocellulosic biomass. Depending on the extraction method, these materials can be categorized into three types: cellulose nanofibrils (CNF)/cellulose microfibrils (CMF), cellulose nanocrystals (CNC)/cellulose microcrystals (CMC), and bacterial cellulose (BC) [5, 29]. Nanocelluloses have a diameter of less than 100 nm [30]. Micro- and nanocelluloses can be classified as cellulosic materials, moderately degraded. This degradation process results in an expanded surface area and is achieved through mechanical disintegration, without the use of hydrolysis [16, 25].

Micro- and nanocelluloses have a wide range of applications in science and technology. They can be used in the production of films, automotive components, biomedical devices, and food. They are also utilized in water treatment and other various applications [1, 18, 31]. Madivoli et al. [32] demonstrated that hybrid antimicrobial composite films, produced with cellulose nanofibrils from sugarcane bagasse, silver nanoparticles, and polyvinyl alcohol can be an excellent alternative to petroleum-based packaging material. Otenda et al. [33] produced starch-hibiscus-cellulose nanofibrils composite films for food packaging. Raghav et al. [34] also studied the application of hybrid AgNPs-carboxyl nanocellulose in active food packaging. Additionally, Rajan et al. [35] reported on the potential use of silane-treated cellulose nanofibers in civil and transportation applications.

The effective separation of biomass components is one of the main challenges in the use of renewable resources. To obtain nanocellulose, it is necessary to isolate the cellulose and prepare nanocellulose from the isolated cellulose [1, 4, 36]. Nano and microcellulose can be produced by mechanically fibrillating them via high-shear microgrinding, microfluidization, high-intensity ultrasonication, or high-pressure homogenization [37]. The steam explosion process [38] and ionic liquids [39] can also be used. Enzymatic treatment and surface modification through catalytic oxidation of the hydroxyl groups using 2,2,6,6-tetramethylpiperidine-1-oxyl (TEMPO) radical to carbonyl groups are commonly used for isolating CNFs [33, 37]. Micro- and nanofibrils obtained by mechanical defibrillation are economically viable [40].

Furthermore, this process does not involve the use of chemicals, making it environmentally friendly.

Other studies have already managed to produce cellulose nanofibrils from coffee parchment. Panyamao et al. [41] used a pretreatment process based on a natural acidic deep eutectic solvent for to isolate cellulose-rich materials from coffee parchment for nanocellulose production. Henao Rodríguez et al. [42] adopted hydrolysis (acid and alkaline) and bleaching to produce cellulose microfibrils from coffee parchment. Reis et al. [38] used parchment fiber to obtain microfibrillated cellulose by the alkaline treatment process followed by a steam explosion assisted by mechanical high shearing. Malarat et al. [43] used ground coffee and produced pulp with alkali treatment (NaOH) and bleaching treatment (acetate buffer solution, sodium chlorite, and water).

Campuzano et al. [44] used ethanol, sodium hydroxide, and hydrogen peroxide to treat ground coffee pulp. Additionally, a bleaching refinement using sodium hypochlorite was carried out to obtain the desired pulp. Currently, the majority of pulps produced worldwide are generated through the kraft process [45]. This process involves the use of sodium sulfide and sodium hydroxide under high pressure and temperature conditions to solubilize lignin and individualize fibers. Kraft pulps can undergo a bleaching process to produce bleached kraft pulps. Wood and other biomass pulps have already been mechanically disintegrated to produce nano- and microcelluloses. However, no reports have been made regarding the production of cellulose micro and nanofibrils from coffee parchment using the kraft process.

The efficient conversion of renewable raw material (coffee parchment) into a product with high added value (MFC) significantly benefits the agro-industrial sector. In addition, it introduces a new alternative fibrous resource, making the coffee agroindustry a more sustainable and competitive sector. The conversion of coffee parchment, a renewable raw material, into a high-value product called MFC, brings significant benefits to the agro-industrial sector. This process not only introduces a new alternative fibrous resource but also makes the coffee agro-industry more sustainable and competitive. However, further research is needed to study the pulps and the production processes of micro- and nanocelluloses. Additionally, it is crucial to emphasize the importance of employing characterization techniques to understand the behavior of particles at the micro- and nanometric scale [36].

The present work utilized the kraft process for chemical delignification, followed by mechanical disintegration to obtain microfibrillated cellulose from coffee parchment. The produced MFCs were then characterized for a better understanding of their physical and chemical properties, which may be useful to guide their potential applications in the future.

2 Material and methods

2.1 Material

The parchment was obtained from the production of *Coffea canephora* in the city of Santa Teresa (19° 55' 53" South, 40° 35' 43" West), Brazil. It is a beige/yellow cartilaginous membrane that surrounds each coffee seed, known as the endocarp. Pulps were obtained from the kraft pulping process of coffee parchment, a residue of the coffee industry.

The kraft process was conducted based on previously optimized parameters to obtain pulps with two kappa numbers, kappa 25, and kappa 60 [46]. Operational conditions for the Kraft process were liquor/biomass ratio (5/1), sulfidity (32%), and residual effective alkali (6–8 g/L) for both kappa numbers. The kappa number 25 used an H-factor of 1140 and effective alkali of 22.5%, while the kappa number 60 used an H-factor of 492 and effective alkali of 20.5%. The pulp with kappa 25 was submitted to an elemental chlorine-free (ECF) bleaching sequence to obtain bleached pulp with a 90% ISO brightness. The bleaching sequence involved oxygen delignification (O₂), chelating (Q), chlorine dioxide (D_{HT} and D), and alkaline extractions with hydrogen peroxide (EP and P) stages, in the order O₂QD_{HT}(EP)DP. The three pulps were then analyzed for contents of carbohydrates (SCAN-CM 71:09) [47], acid-soluble lignin (TAPPI UM250) [48], acid-insoluble lignin (TAPPI T222 om-02) [48], uronic acids [49], and hexenuronic acids (TAPPI T282 pm-07) [48], and used for the production of microfibrillated cellulose.

2.2 Production of microfibrillated celluloses (MFC)

The MFC suspensions were produced at the Center of Technology for the Chemical and Textile Industries (Senai CET-IQT, Rio de Janeiro, Brazil). Defibrillation was performed in a SuperMassColloider ultra-refiner (MKZA10-15 J IV, Masuko). The disks used in this process (model MKE10-46) are made of ceramic material (aluminum oxide and resin) without porosity to avoid any infiltration of nanometric particles and to allow a better fit between the disks.

The cellulosic pulp suspension used for the production of MFC was prepared by adding 150 g (dry basis) of cellulosic pulp to 9516.13 g of water, as the dry content of the cellulosic pulp was 31%. In other words, 483.87 g of cellulosic pulp (wet basis) was dispersed in 9516.13 g of water, resulting in a total of 10 L of suspension. More precisely, 150 g (dry basis) of each pulp was weighed and dispersed in 50% of the total deionized water. The suspension was left to stand for 72 h to allow for the complete hydration of the pulp. Then, the additional volume of water needed to reach a total volume of 10 L was added. The suspension was stirred for

2 h at a rotation speed of 650 rpm, using a mechanical stirrer (Heidoph). It is important to note that there are no losses during the MFC production process, so the concentration of MFC is assumed to be the same as the concentration of the cellulosic pulp suspension (which was confirmed through moisture content analysis).

During the defibrillation process, one of the disks remained stationary and the other was in motion (1500 rpm). The distance between the disks was set at 100 μm and 32 cycles were performed for each of the three suspensions. The initial position was determined by the noise generated by the contact between the disks, before loading the suspension. From this position, the ultra-refiner was loaded with the cellulosic suspension, and the disks were immediately adjusted to the desired distance. The ultra-refiner was operated with a cooling system using water flow at room temperature.

2.3 Characterization of microfibrillated celluloses

The produced MFCs were analyzed for the contents of carbohydrates (SCAN-CM 71:09) [47], acid-soluble lignin (TAPPI UM250) [48], acid-insoluble lignin (TAPPI T222 om-02) [48], uronic acids (Scott, 1979) [49], hexenuronic acids (TAPPI T282 pm-07) [48], ash (TAPPI 211 om-08) [48], and silica (TAPPI T245 cm-98) [48].

The analysis of viscosity was performed according to the dynamic viscosity technique, using the Viscometer from Lamy Rheology. The spindle R4 was coupled to the viscometer with the rotation set at 20 rpm and the temperature was controlled at 25 $^{\circ}\text{C}$ using a water bath. The torque was measured simultaneously with the viscosity measurements, as recommended by the manufacturer. Each viscosity analysis was conducted for 360 s. Fiber analysis was performed using the Valmet FS5 Analyzer, in order to obtain length and diameter dimensions. The samples were suspended in demineralized water for analysis.

The elemental composition, including carbon, hydrogen, nitrogen, and sulfur percentages, was determined using the LECO TruSpec CHNS Micro module, which is part of the CHNS-O model equipment. The percentage of oxygen was determined by the difference method. The combustion tube was maintained at a temperature of 1050 $^{\circ}\text{C}$. Following combustion, the gases were transported to the reduction tube and then to the detection column. Independent infrared detectors were used for simultaneous detection of carbon, hydrogen, and sulfur, while nitrogen was measured using a thermal conductivity detection system.

X-ray diffraction was performed using a Panalytical-Aeris Cu-Ka diffractometer ($\lambda = 154,056 \text{ \AA}$). Films with a grammage of 30 g/m^2 were formed and dried at room temperature for 48 h. The adopted configuration was the slit monochromator mode, operating at 40 kV with a current of 30 mA. The scan range was set at 0–30 $^{\circ}$ and continuous scans were

performed for the θ –2 θ range at a scan speed of 3 min^{-1} , using Cu-Ka radiation with a wavelength of 0.154 nm. The crystallinity index was determined according to the method proposed by Segal et al. [50] using the ratio between the maximum intensity of diffraction and the minimum intensity located between the two crystalline peaks of the diffractogram (Eq. 1), where I_{002} is the maximum diffraction intensity, attributed to the crystalline regions (2θ between 22 and 23 $^{\circ}$) and I_{AM} is the minimum intensity, assigned to non-crystalline regions (2θ between 18 and 19 $^{\circ}$).

$$CI (\%) = \frac{I_{002} - I_{AM}}{I_{002}} \times 100 \quad (1)$$

The thermogravimetric analyses were performed using a Hitachi thermal analyzer (model STA 7300). Films weighing 30 g/m^2 were formed and dried at room temperature for 48 h. The analyses were performed under a nitrogen gas atmosphere, at a constant flow rate of 50 mL/min. Thermogravimetric (TG) curves were obtained from 25 $^{\circ}\text{C}$ to a maximum temperature of 800 $^{\circ}\text{C}$. The heating rate was 10 $^{\circ}\text{C}/\text{min}$, conducted in an inert atmosphere. Thermal degradation was obtained through the first derivative of the TG curve, which quantifies the mass loss as a function of temperature.

Fourier-transform infrared spectroscopy (FTIR) was performed using a Bruker Vertex 80 FTIR spectrophotometer, with the attenuated total reflection (ATR) configuration. Films with a grammage of 30 g/m^2 were formed and dried at room temperature for 48 h. The analyses were performed at room temperature, with a wavelength ranging from 400 to 4000 cm^{-1} and 32 scans per spectrum at a resolution of 4 cm^{-1} .

Zeta potential was measured using the Litesizer 500 equipment from Anton Paar. The samples of MFC were diluted in distilled water to a consistency of 0.1% (w/w) and homogenized in a mechanical agitator at 200 rpm for 60 min. The analysis was performed at 25 $^{\circ}\text{C}$ and the refractive index of water was used for calibration.

Water retention value (WRV) was performed according to the TAPPI UM-256 standard [48]. The WRV indicates the capacity of fibers to swell and absorb water, and it was calculated according to Eq. 2. W_{humid} is the weight of the sample after centrifugation and W_{dry} is the dry weight of the sample.

$$WRV (\%) = \frac{W_{humid} - W_{dry}}{W_{dry}} \times 100 \quad (2)$$

Scanning electron microscopy (SEM) of the MFC samples was performed using a scanning electron microscope model JSM610LV. The operating parameters were set to 20 kV voltage and filament current of 81.2 μA . In order to improve the electrical conductivity and minimize the effect of surface charge during analysis, the samples were

freeze-dried and coated with a thin layer of gold using a metallizer. The metallization process lasted for 2 min, resulting in a gold layer of approximately 60 nm thickness on the samples.

3 Results and discussion

3.1 Production of microfibrillated celluloses (MFCs)

Images of the pulp before and after defibrillation are presented in Fig. 1. Microfibrillated cellulose (MFC) can be considered as a cellulosic material, that is fibrillated, resulting in an expanded surface area. It can be obtained through a mechanical disintegration process without the use of hydrolysis [16].

To verify the variations inherent to the mechanical system of the defibrillation process in relation to the characteristics of each cellulosic pulp, the three obtained suspensions were prepared and defibrillated in the SuperMassColloider under the same conditions of suspension consistency, disc rotation, distance between discs, and number of passes. The obtained MFCs were identified as MFLC-K#25, MFLC-K#60, and MFC-Bleached, from K#25, K#60 and bleached pulps, respectively.

The yields were not measured in this work. However, it is known that the number of passages through the mill and the use of pulps with or without residual lignin can affect the final result, due to the loss of fibers during the bleaching process. Ribes et al. [51] obtained a yield of 99.39% and 98.13% for nanofibril suspensions of *eucalyptus* pulps with and without residual lignin, respectively. Reis et al. [38] reported that the yield of MFC obtained after consecutive treatments was 20.5 g MFC/100 g of dried parchment (PAR).

3.2 Characterization of microfibrillated celluloses

3.2.1 Fiber size and viscosity

The dimensions of the fibers (length and diameter) and viscosity of the MFCs are presented in Table 1. Changes in the size distribution profile were expected throughout the defibrillation process, especially in the longitudinal direction of the fiber [52]. Another anticipated outcome was the attainment of highly viscous suspensions, even at very low consistencies [25].

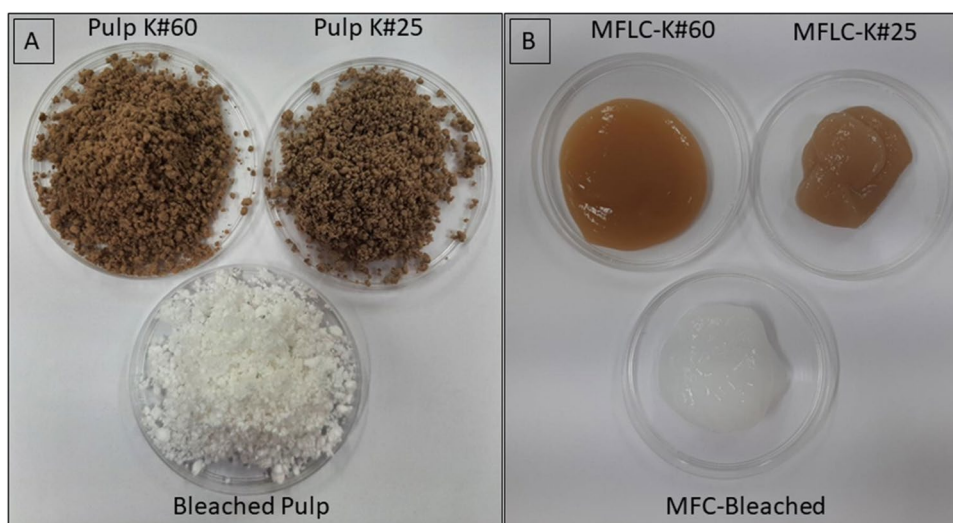
Nanocelluloses generally present a diameter in the range of 20 to 100 nm and a length of several micrometers [25, 53, 54]. The length of several micrometers measured in this study ranged from 39 to 47, and the measured diameters (nm) were 6820 (MFLC-K#60), 5600 (MFLC-K#25), and 5280 (MFC-Bleached). In this study, the mechanical process allowed for the production of micrometers in diameter, hence the material was named microcelluloses. Malarat et al. [43] obtained nanocellulose (NCP) from coffee pulp in the form of cellulose nanocrystals with a diameter of 16.03 ± 4.70 nm.

Henao Rodríguez et al. [42] used hydrolysis (both acid and alkaline) and bleaching techniques to extract cellulose microfibrils from coffee parchment. The researchers determined that the microfibrils obtained from acid hydrolysis had a size of 8 ± 2 μm , while those obtained

Table 1 Evaluation of microfibrillated celluloses as to their dimensions and viscosity

Parameters	MFLC-K#60	MFLC-K#25	MFC-Bleached
Length, μm	39	47	47
Diameter, nm	6820	5600	5280
Viscosity, cP	5357	8336	15,587

Fig. 1 Pulp before and after defibrillation: **A** kraft pulps and **B** microfibrillated celluloses



from alkaline hydrolysis had a size of $27 \pm 2 \mu\text{m}$. The bleaching process resulted in microfibrils with a size of $23 \pm 2 \mu\text{m}$. Additionally, the authors employed the term “microcelluloses” to refer to these extracted materials.

The instrument used for fiber measurement, the Valmet FS5 Analyzer, considered that 98.2–99.5% of the MFC suspension consisted of smaller fiber particles known as fines. As a result, only 0.5–1.8% of the samples were subjected to length and diameter measurements, as the dimensions of the fines did not accurately represent the MFCs. Mechanical defibrillation produces a diverse material that contains fibers, fiber fragments, fines, and fibrils [55, 56].

The delignification and bleaching processes lead to pulps with varying amounts of hemicelluloses and lignin. Additionally, the degree of polymerization and crystallinity of cellulose is reduced, which affects the properties of microfibrils [25, 57]. For instance, microfibrillated lignocellulose (MFLC) derived from unbleached pulps has longer fibers and produces less viscous suspensions compared to MFC obtained from bleached pulps [25, 58]. These findings are consistent with the results presented in Table 1 of the current study.

The viscosity of the MFC was measured to be 15,587 cP at a solids content of 1.5%. The high viscosity is related to the hygroscopic nature of the cellulose, as well as the high aspect ratio and specific surface area of the microfibrils. As a result, it was anticipated that the fibers in the MFC suspension would exhibit stronger interactions, leading to the formation of highly viscous suspensions [25].

3.2.2 Chemical composition

The chemical composition of the pulps and MFC suspensions is shown in Table 2. The suspensions presented a chemical composition that is similar to the original pulps because they were produced through a purely mechanical process. Unbleached pulps had a higher proportion of lignin

than bleached pulp. The main objective of bleaching is to remove residual lignin and produce pulp with a brightness of 90%ISO.

Mechanical fibrillation affects the size of fibers, without changing their chemical components [25]. However, Jiang et al. [59] and Carvalho et al. [60] explain that as the fibrillation degree increases, lignin migrates out of the fibrils. This leads to the separation of lignin from microfibrils, which modifies their composition. Additionally, residual lignin affects the polarity and hydrophilicity of microfibrillated cellulose. Lignin has a lower polarity compared to carbohydrates [61, 62]. These changes in properties expand the potential applications of microfibrillated cellulose.

The mechanical degradation showed a small reduction in the amount of lignin in MFCs, compared to pulps. It was observed that the higher the kappa number in the original pulp, the higher the content of lignin and hexenuronic acids (HexA) in the MFC suspension. Lignin and HexA are known to contribute to the measurement of the kappa number [63]. The total lignin contents for MFLC-K#60, MFLC-K#25, and MFC-Bleached samples were 9.34%, 3.04%, and 0.43%, respectively. HexA contents observed for MFLC-K#60, MFLC-K#25, and MFC-Bleached samples were 1.20%, 1.10%, and 0.04%, respectively.

Higher percentages for glycans and xylans were also observed. Eucalypt and coffee, classified as hardwoods, have xylan as the main hemicelluloses [64]. Coura et al. [46] reported the chemical composition of coffee parchment as follows: 36.8% glucan, 20.6% xylan, 0.4% mannan, 0.5% galactan, and 0.2% arabinan. This indicates the presence of other hemicelluloses in parchment. However, these carbohydrates are extensively degraded during kraft pulping, which justifies the absence or low content of mannan, galactan, and arabinan in pulps and microfibrillated celluloses. In a study by Demuner et al. [65], nanocellulose samples produced from eucalyptus kraft pulp showed glycans and xylans percentages of 80.6% and 13.8% for

Table 2 Characterization of kraft parchment pulps and MFC suspensions

Constituents	Pulps			Microfibrillated celluloses			
	K#60	K#25	Bleached	K#60	K#25	Bleached	
Acid-soluble lignin, %	0.93	0.78	0.46	0.84	0.64	0.43	
Acid-insoluble lignin, %	8.75	2.49	-	8.50	2.40	-	
Total lignin, %	9.68	3.27	0.46	9.34	3.04	0.43	
Uronic acids, %	1.70	1.31	0.90	1.60	1.25	0.87	
Hexenuronic acids, %	1.20	1.10	0.04	1.20	1.10	0.04	
Sugars, %	Glucan	62.40	67.30	64.40	64.40	67.50	70.80
	Xylan	20.70	21.70	19.20	19.20	20.30	22.10
	Mannan	0.00	0.00	0.00	0.00	0.00	0.00
	Galactan	0.10	0.20	0.10	0.10	0.10	0.10
	Arabinan	0.00	0.10	0.00	0.00	0.10	0.10

lignocellulose nanofibrils (LCNF) and 83.3% and 14.2% for cellulose nanofibrils (CNF), respectively. The other sugars were between 0.0 and 0.3%.

Malarat et al. [43] conducted a study where pulp was produced from coffee using alkali treatment (NaOH) and bleaching treatment. They also produced nanocelluloses from coffee pulp (NCP) through acid hydrolysis. In the pulp treated with NaOH, the authors observed that cellulose, hemicelluloses, lignin, and ash accounted for 76.32%, 5.87%, 10.98%, and 0.14%, respectively. In the bleached pulp, the percentages of cellulose, hemicelluloses, lignin, and ash were 85.83%, 3.71%, 1.56%, and 0.04%, respectively. These findings indicate that the process used to prepare the pulp has an impact on the chemical characteristics of the resulting microcelluloses.

The glycan and xylan contents for MFLC-K#60, MFLC-K#25, and MFC-Bleached were 64.4 and 19.2%, 67.5 and 20.3%, and 70.8 and 22.1%, respectively. In all samples, we observed a higher xylan content and lower glycan content. This result can be explained by the difference in the chemical composition of the used raw material [38, 66, 67]. Hemicelluloses are known to help the nanofibrillation by facilitating the release of individual fibrils, thereby reducing energy consumption during mechanical defibrillation [68].

The proportion of sugars increases as the other components decrease. MFC-Bleached contains higher percentages of sugars due to the removal of lignin and HexA during the bleaching process. The higher levels of sugars in the MFLC-K#25, compared to MFLC-K#60, can be explained by the more drastic process used to achieve a kappa number of 25, resulting in lower levels of lignin and HexA.

The contents of HexA ranged from 0.04 to 1.20%, and the contents of uronic acids ranged from 0.87 to 1.60%. A higher amount of residual lignin was observed in the raw material due to its chemical composition. Although coffee has lower lignin content (10.1–26.6% compared to 27.1–31.3% in eucalyptus wood), its S/G lignin ratio (the ratio of lignin syringyl units to guaiacyl units) is 0.8. In contrast, studies report values of 2.5–3.1 for eucalyptus wood [69–71].

This S/G lignin ratio and the associated linkages between the units are crucial as they impact the reactivity of lignin during pulping [72]. The S-type lignin, with two methoxyl groups in the C-3 and C-5 positions of the aromatic ring, is more reactive [72], whereas G-type lignin, with the C-5 position available for carbon–carbon bonding, contributes to a higher degree of lignin condensation [73, 74].

MFC samples primarily consist of organic compounds (cellulose, hemicelluloses, and lignin) with a small percentage of inorganic compounds, which can be quantified through ash content analysis [75]. MFLC-K#60, MFLC-K#25, and MFC-Bleached presented ash values ranging from 0.85 to 1.63%, reflecting the characteristics of the raw

material's chemical composition (Table 3). Coffee parchment generally contains higher ash content (0.5–7%) compared to eucalyptus wood (0.1–0.3%) [38, 67, 69, 71]. The silica content was 0.41% in MFLC-K#60 and absent in MFLC-K#25 and MFLC-Bleached.

Elemental analysis of lignocellulosic biomass reveals that carbon, oxygen, and hydrogen are the main elements present (Table 3). These elements are found in organic substances like cellulose, hemicelluloses, and lignin [75, 76]. Sulfur and nitrogen are present in lower proportions, and may come from the protein residues present in coffee parchment [69, 77]. Sulfur could also be present due to the kraft pulping process, which utilizes sodium sulfide as a reagent.

3.2.3 X-ray diffraction (XRD)

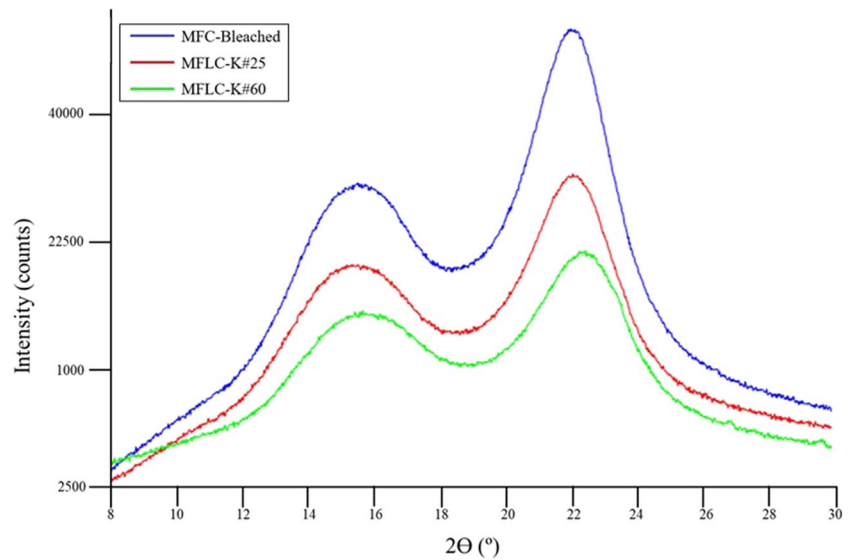
X-ray diffraction (XRD) analysis was performed to determine the crystallinity of the MFLC and MFC samples, using the Segal empirical method, which employs the height of the main diffraction peak, referred to the crystallographic plane (200). The diffractogram presented in Fig. 2 shows diffraction intensity peaks around 18.2–18.8 for the amorphous peaks (I_{AM}) and 21.8–22.2 for the crystalline peaks (I_{002}), indicating that the samples present the typical polymorph of cellulose type-I. According to Ass et al. [78], the peak referring to the crystalline fraction at $22^\circ \leq 2\theta \leq 23^\circ$ corresponds to cellulose type-I, while for cellulose type-II this peak occurs at $18^\circ \leq 2\theta \leq 22^\circ$. In terms of the regions corresponding to the amorphous fraction, for type-I and type-II, they occur at $18^\circ \leq 2\theta \leq 19^\circ$ and $13^\circ \leq 2\theta \leq 15^\circ$, respectively. Li et al. [79] stated that the main distinction between cellulose I and II is the antiparallel chain arrangement in the latter.

The crystallinity of microfibrillated cellulose increases by the successive dissolution of lignin and hemicelluloses during the pulp extraction step [4]. The delignification and bleaching processes affect the raw material by modifying the content of hemicelluloses and lignin, reducing the degree of polymerization and crystallinity of the cellulose [25]. The percentage of lignin, hemicelluloses,

Table 3 Inorganic composition and elemental analysis of MCF samples

Parameters, %	MFLC-K#60	MFLC-K#25	MFC-Bleached	
Silica	0.41	0.00	0.00	
Ash	1.63	1.19	0.85	
Elemental analysis	C	49.10	46.30	46.30
	H	6.18	6.34	6.20
	N	0.06	0.02	0.05
	S	0.17	0.16	0.15
	O	44.49	47.18	47.30

Fig. 2 X-ray diffractogram of the MFC suspensions



and cellulose varies in the produced MFCs, resulting in a varied distribution of the crystalline and amorphous components.

The crystallinity values were 52.5%, 58.8%, and 65.1% for the MFLC-K#60, MFLC-K#25, and MFC-Bleached samples, respectively. Raju et al. [80] achieved 82.31% crystallinity for nanofibres of *E. tereticornis*. Oliveira [81] reported 81.3% crystallinity for eucalyptus fibers, and 49.1% and 53.6% for unbleached and bleached coffee husk fibers, respectively. Campuzano et al. [44] reported a crystallinity of 75% for coffee parchment regenerated cellulose nanoparticles (RCNPs). On the other hand, Malarat et al. [43] reported a crystallinity index (CI) of 80.55% for nanocellulose from coffee pulp. This CI is higher than what was found in this study, primarily because the chemical process employed by Malarat et al. removed the amorphous regions, leading to a higher crystallinity index.

The difference in crystallinity between eucalyptus and coffee parchment can be attributed to the characteristics of each biomass. The coffee parchment pulp contains more lignin and hemicelluloses, and less cellulose, compared to eucalyptus pulp. This means that it has a higher proportion of amorphous components and a lower proportion of crystalline components in its composition.

3.2.4 Thermogravimetric analysis (TG/DTG)

Thermogravimetric analysis (TGA) is a crucial technique for understanding the thermal stability and decomposition behavior of materials, including MFC suspensions. This technique involves monitoring changes in the mass of a

sample over time or temperature, which can be caused by physical processes like sublimation, evaporation, or condensation, as well as chemical processes like degradation, decomposition, or oxidation.

Thermal degradation occurs in three phases. The first phase occurs around 60–100 °C, during which the water absorbed on the surface of the microfibrillated cellulose and volatile compounds of low molar mass are generally released [4, 82]. The degradation peak of the second phase appears around 250–350 °C, depending on the size and length of the MFC. At this stage, the material starts to degrade, which usually depends on several factors, such as the nature of the feedstock [4, 82]. After 350 °C, the mass loss gradually decreases with increasing temperature, when the volatilization of the components is complete and any additional mass loss is related to the degradation of the residual coal. Moreover, an increase in temperature above 450–600 °C leads to complete degradation of the sample [4].

The thermal stability of MFLC and MFC is an important parameter for their use as reinforcing agents in thermoplastic materials, which typically require processing temperatures above 200 °C [38]. To assess the thermal stability of the prepared MFCs, thermogravimetric (TGA) analysis was performed. Figure 3 displays the resulting thermogravimetric curves, indicating the mass loss with respect to temperature, as well as the first derivative of TG (DTG) curves, showing the change in mass over time as a function of temperature.

The degradation curves obtained from the three MFC suspensions can be characterized by several key parameters, which provide insights into their thermal properties (Table 4): the temperature at which the thermal degradation

Fig. 3 TG/DTG curves of the MFC suspensions

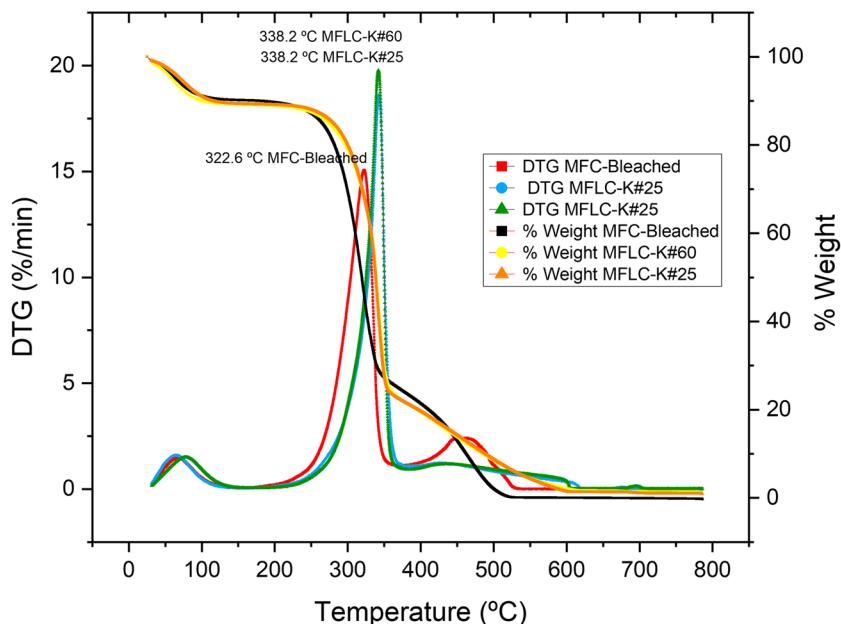


Table 4 Marked temperature peaks during thermal degradation and residual ash content

Samples	Thermal degradation ranges (°C)				Residual ash content (%)
	Tonset	T50%	Tmax	Tendset	
MFLC-K#60	271.8	333.8	338.2	414.7	2.16
MFLC-K#25	275.0	333.6	338.2	405.9	1.51
MFC-Bleached	265.8	319.4	322.6	347.1	0.05

began (Tonset), the temperature at which 50% mass loss of the analyzed sample occurred (T50%), the maximum degradation temperature, the final temperature of the thermal composition (Tendset), and the residual ash content. It was observed that the maximum degradation temperatures (Tmax), which generally reflect the point at which the maximum decomposition rate of the sample components occurs, were higher for MFLC-K#60 (338.2 °C) and MFLC-K#25 (338.2 °C) compared to MFC-Bleached (322.6 °C). In the thermogravimetric analysis, the mass loss between 200 and 350 °C is associated with the degradation of hemicelluloses and the beginning of cellulose degradation [83]. According to Table 2, samples MFLC-K#25 and K#60 present similar chemical compositions, especially in terms of

hemicelluloses and cellulose content, which may result in similar thermal profiles in TGA and equal Tmax value.

The analysis reveals that MFLCs are more thermally stable compared to MFCs, which is consistent with previous studies. Reis et al. [38] reported a Tmax of 330 °C for coffee parchment, attributed to the presence of lignin, which is known for its higher thermal resistance compared to hemicelluloses and cellulose [84]. Therefore, the improvement in thermal stability of MFLCs can be explained by the presence of lignin in their chemical composition, which contributes to the higher Tmax temperatures observed in thermogravimetric analyses.

Campuzano et al. [44] and Henao Rodríguez et al. [42] reported a similar thermal profile for coffee parchment regenerated cellulose nanoparticles (RCNPs) and cellulose microfibrils extraction from coffee parchment, respectively.

The significant mass loss of MFCs occurred in the range of 300–400 °C (Table 5). This mass loss is attributed to the dehydration of cellulose and thermal depolymerization of this polymer [84]. MFC-Bleached lost more mass in the 200–300 °C range when compared to MFLC, which can be explained by the chemical composition. Generally, the thermal degradation of cellulose occurs later than that of hemicelluloses, due to the greater amount of energy required for

Table 5 Temperature ranges for loss of mass of the samples

Samples	Loss of mass (%)				
	100–200 °C	200–300 °C	300–400 °C	400–500 °C	500–600 °C
MFLC-K#60	1.15	10.89	58.78	11.02	6.05
MFLC-K#25	1.83	9.55	59.82	10.95	7.26
MFC-Bleached	1.44	20.31	47.98	19.34	2.05

depolymerization of the cellulose chain and for the breakdown of its monomers.

The crystallinity index (CI) represents the proportion of cellulose that is organized into crystalline domains. It is believed that cellulose crystallinity can vary according to the initial content of amorphous structures (hemicelluloses and lignin) [65, 83]. In other words, the breakdown of amorphous regions contributes to the increase in CI. On the other hand, higher hydrolysis values lead to a decrease in both molecular weight and T_{max} values. This can be attributed to the hydrolysis effect on the crystalline part of cellulose as well as the amorphous regions [85, 86]. Berto et al. [83] demonstrated that a material with a lower CI also exhibited a reduction in Tonset. The contrasting behavior observed in the MFC-Bleached sample may be related to particle size. In addition to CI, it is expected that the thermal stability could be influenced by the morphological aspect of the particles, such as their size and surface area. This is because smaller particle sizes result in larger surface areas exposed to heat [83].

3.2.5 Fourier transform infrared spectroscopy (FTIR)

FTIR analysis is a valuable tool for identifying the functional groups and bonds in cellulose. It was used in this study to determine potential changes in the functional groups of microcellulose fibers. In the case of microfibrillated cellulose samples, the infrared profiles showed similar patterns with distinct bands (Fig. 4), corresponding to the stretching and deformation of C-H, O-H, and C-O.

Cellulose is composed of various bonds, including C-C, C-H, and C-O-C, as well as hydroxyl groups (-OH) on its surface. The band at 3330 cm⁻¹ is attributed to the broad stretching and bond vibration of O-H and absorbed water, which includes hydrogen bonding. The band at 2890 cm⁻¹ corresponds to the vibration of C-H bonds, specifically CH and CH₂, which are present in both cellulose and hemicelluloses [39, 82, 87, 88]. The stretching of carboxylic acid

bonds, such as C=O and C-O, which are found in hemicelluloses, can be observed at 1635 cm⁻¹ [87, 88].

The vibration of the aromatic ring in lignin is attributed to 1559 cm⁻¹ [37]. The deformation of the symmetric bond of the CH and CH₂ groups of cellulose and hemicelluloses is represented by 1428 cm⁻¹ [87]. The angular deformation of C-O bonds of primary alcohols in cellulose and hemicelluloses, as well as the C-O-C bonding of asymmetric 1,4-glycosidic bonds of D-glucose, were assigned to 1116 and 1027 cm⁻¹ [4, 38], respectively. The β-Glycosidic linkages between cellulose glucose units are represented by 895 cm⁻¹ [88].

Although the wavenumbers of the functional groups align across the samples, the peak intensity may vary due to differences in raw materials and methods employed [4]. In the MFLC samples (K#60 and K#25), a peak at 1559 cm⁻¹ was observed due to the presence of the aromatic ring in lignin. This peak was not evident in the MFC sample (Bleached).

Malarat et al. [43] characterized nanocelluloses from coffee pulp (NCP) produced via acid hydrolysis and highlighted the bands at 3330, 2920–2848, and 1025 cm⁻¹. Campuzano et al. [44] characterized regenerated cellulose nanoparticles (RCNPs) from coffee parchment through mechanical, centrifugation, and dialysis into cellulose membranes processes. The authors observed bands at 3325, 2890, 1624, 1420, 1159, 1039, and 895 cm⁻¹, similar to those found in this study.

3.2.6 Zeta potential

Zeta potential is a characterization that evaluates the colloidal stability of suspensions, taking into account the density of surface charges. The stability of suspensions is directly linked to the surface forces of particles and the interactions between them (repulsion or attraction). The strength of these characteristics defines the formation of particle clusters in suspension and their sizes, leading to sedimentation [89, 90].

Both the stability and electrostatic repulsion between the fibers increase as the zeta potential decreases. Usually,

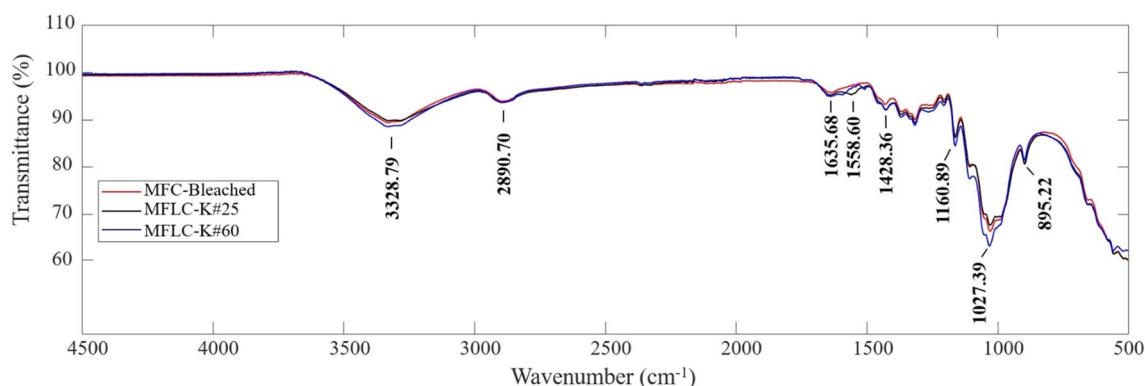
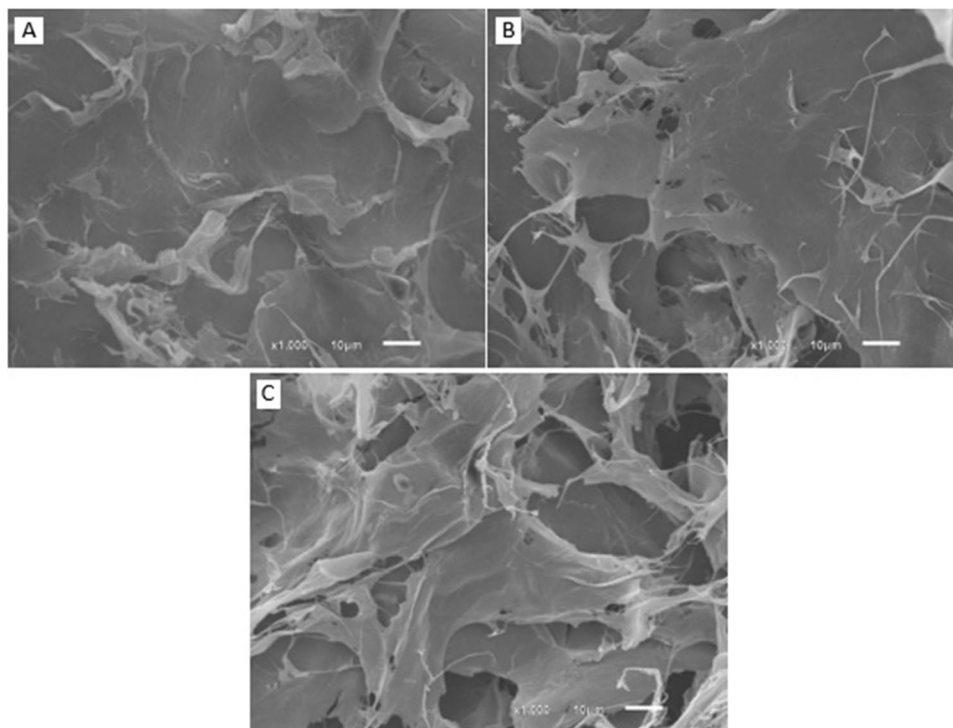


Fig. 4 FTIR spectra of the MFC suspension samples

Fig. 5 SEM images at $\times 1000$ magnification—10 μm : **A** MFLC-K#60 and **B** MFLC-K#25 and **C**) MFC-Bleached



the system is considered moderately stable when it is lower than -30 mV [90]. On the other hand, values between 10 and 30 are considered unstable [89]. The zeta potential values obtained for MFLC-K#60, MFLC-K#25, and MFC-Bleached were -19.8 mV, -15.8 mV, and -27.4 mV, respectively. The results showed that the MFC-Bleached is the best in terms of colloidal stability and the MFLC-K#25 sample is the most unstable.

Several factors can influence the zeta potential, including the length of microfibrils, which can lead to the interlacing of MFLC and MFC. The presence of residual hemicelluloses due to their binding capacity, and the sulfur content, which increases surface charges, are also important factors [91].

To improve the fibrillation and quality of the suspension, the carboxyethyl reaction can be used as a pretreatment method for MFC preparation. Chen et al. [92] worked with bleached acacia kraft pulp and performed carboxyethyl pretreatment of pulp fibers. They fibrillated the fibers using a Supermasscolloider Type Disk mill to prepare microfibrillated cellulose (MFC). The results showed that the charge density, suspension stability, and transparency of MFC increased with the presence of carboxyethyl groups.

3.2.7 Water retention value (WRV)

The water retention value presents a measure of the fibers' ability to absorb water, after centrifugation under standard

conditions. This property is associated with the binding capacity of the fibers, since they have exposed free hydroxyl groups, and a larger surface area [17, 93, 94].

The WRV values for MFLC-K#60, MFLC-K#25, and MFC-Bleached were 792, 849, and 1032%, respectively. The different values obtained by the samples can be justified by their chemical compositions (Table 2). Xylans, which have negatively charged carboxylic groups, contribute to higher WRV [95]. On the other hand, a higher lignin content reduces the WRV due to its hydrophobic nature [57].

Demuner et al. [65] found higher WRV values for eucalyptus nanofibrils (1117% for LCNF and 1496% for CNF) compared to MFCs from coffee parchment. This difference can be explained by the smaller size and larger surface area of eucalyptus nanofibrils, which enhance water retention [96].

3.2.8 Scanning electron microscopy (SEM)

Scanning electron microscopy is a useful technique for analyzing the surface of nanomaterials... By examining these images, it is evident that the fiber walls have been deconstructed through the mechanical process of defibrillation, thereby releasing the microfibrils from the interior of the fibers.

The pulp used for the production of MFLC-K#60 was obtained using milder kraft cooking conditions, which resulted in better preservation of the pulp compared to K#25 pulps. In the case of the bleached pulp sample, the fibrils

are more exposed due to the bleaching process (Fig. 5C). Henao Rodríguez et al. [42] also observed differences in SEM images of cellulose microfibrils extracted from coffee parchment that underwent different treatments.

4 Conclusions

Cellulose fibers derived from coffee industry residues (parchment) can be utilized to produce microfibrillated cellulose (MFC) and microfibrillated lignocellulose (MFLC), which exhibit comparable properties to microcelluloses produced from eucalypt.

The microfibrillated celluloses had a high content of lignin and hemicelluloses, which contributed to a reduction in their crystallinity. Specifically, MFLC-K#60, MFLC-K#25, and MFC-Bleached showed crystallinity indexes of 52.5, 58.8, and 65.1%, respectively. All the three samples demonstrated thermal stability, with MFLC-K#60 having a maximum degradation temperature of 339 °C, MFLC-K#25 of 339 °C, and MFC-Bleached of 322 °C.

The FTIR spectra were similar for all microfibrillated celluloses, showing peaks characteristic of cellulosic polymers. However, MFLC exhibits distinctive peaks associated with lignin, which are absent in MFC. Zeta potential values found for MFLC-K#60, MFLC-K#25, and MFC-Bleached samples are -19.8 mV, -15.8 mV, and -27.4 mV, respectively. The suspensions of MFCs are unstable and present the tendency to agglomerate. Scanning electron microscopy confirmed that the fibers are deconstructed due to the mechanical defibrillation process in all three samples.

The characterization of MFLC and MFC is quite similar, making MFLC more advantageous when a colorless suspension is not required or when the presence of lignin contributes to the desired product, such as in sunscreens where lignin aids in UV protection. Additionally, the production cost of MFLC is lower than that of MFC due to the lower alkali load and less drastic pulping conditions, resulting in a higher yield. Moreover, the production of MFLC eliminates the need for the bleaching step used to remove residual lignin present in the pulp from the cooking process.

Acknowledgements We are thankful for the funding from Minas Gerais State Research Foundation (FAPEMIG), from the Brazilian National Council for Science and Technology Development (CNPq), Embrapa Consórcio-Café, Coordination for the Improvement of Higher Education Personnel (CAPES) is greatly appreciated. We are grateful for the partnership with the Technology Center for the Chemical and Textile Industries (Senai CETIQT).

Author contribution Marcela Coura: conceptualization, investigation, methodology, visualization, writing original draft. Antonio Demuner: resources, writing review and editing, funding acquisition. Robisnea Ribeiro: data curation, writing review and editing. Lara Demuner: investigation, writing review and editing. Julia Figueiredo: investigation, writing review & editing. Fernando Gomes: data curation, writing

review and editing. Verônica Barbosa: investigation, methodology. Maria Firmino: investigation, methodology. Ana Carvalho: writing review and editing. Daiane Blank: investigation, methodology. Marcelo Santos: conceptualization, writing review and editing.

Declarations

Conflict of interest The authors declare no competing interests.

References

1. Franco TS, Potulski DC, Viana LC et al (2019) Nanocellulose obtained from residues of peach palm extraction (*Bactris gasipaes*). *Carbohydr Polym* 218:8–19. <https://doi.org/10.1016/j.carbpol.2019.04.035>
2. Joseph TM, Unni AB, Joshy KS et al (2023) Emerging bio-based polymers from lab to market: current strategies, market dynamics and research trends. *C (Basel)* 9:30. <https://doi.org/10.3390/c9010030>
3. Khatun B, Das J, Rizwana S, Maji TK (2023) Biodegradable polymers- a greener approach for food packaging. In: *Green Sustain Process Chem Environ Eng Sci*. Elsevier, pp 317–369. <https://doi.org/10.1016/B978-0-323-95644-4.00010-3>
4. Marakana PG, Dey A, Saini B (2021) Isolation of nanocellulose from lignocellulosic biomass: synthesis, characterization, modification, and potential applications. *J Environ Chem Eng* 9:106606. <https://doi.org/10.1016/j.jece.2021.106606>
5. Owolabi FAT, Deepu AG, Thomas S et al (2020) Green composites from sustainable cellulose nanofibrils. In: *Encyclopedia of Renewable and Sustainable Materials*. Elsevier, pp 81–94. <https://doi.org/10.1016/b978-0-12-803581-8.11422-5>
6. Setter C, Borges FA, Cardoso CR et al (2020) Energy quality of pellets produced from coffee residue: characterization of the products obtained via slow pyrolysis. *Ind Crops Prod* 154:112731. <https://doi.org/10.1016/j.indcrop.2020.112731>
7. Ferreira LT, Cavaton T (2023) Produção mundial de café. <https://www.embrapa.br/busca-de-noticias/-/noticia/77745125/producao-mundial-de-cafe-foi-estimada-em-1672-milhoes-de-sacas-de-60kg#:~:text=socioecon%C3%B4micos%20e%20ambientais,Produ%C3%A7%C3%A3o%20mundial%20de%20caf%C3%A9%20foi%20estimada%20em%20167,milh%C3%B5es%20de%20sacas%20de%2060kg&text=setembro%20de%202023-,A%20previs%C3%A3o%20total%20da%20produ%C3%A7%C3%A3o%20de%20do%20consumo%20de%20caf%C3%A9,a%20se%20manter%20relativamente%20est%C3%A1veis>. Accessed 9 Jul 2024
8. ReportLinker (2024) Brazil coffee market overview 2024–2028. https://www.reportlinker.com/market-report/Soft-Drink/464/Coffee?term=coffee%20market&matchtype=b&loc_interest=&loc_physical=1001592&utm_group=standard&utm_term=coffee%20market&utm_campaign=ppc&utm_source=google_ads&utm_medium=paid_ads&utm_content=transactionnel-1&hsa_acc=9351230540&hsa_cam=15072746546&hsa_grp=126923822301&hsa_ad=563625669011&hsa_src=g&hsa_tgt=kwd-407845236150&hsa_kw=coffee%20market&hsa_mt=b&hsa_net=adwords&hsa_ver=3&gad_source=1&gclid=CjwKCjwKcAjw4ri0BhAvEiwA8oo6F7fJlVlAEoxKe6AplIWGJ23aLjJ5wXCmuNw85ZnPheZs0g1ykTYtdRoCzQMqAvD_BwE. Accessed 31 Jul 2024
9. Esquivel P, Jiménez VM (2012) Functional properties of coffee and coffee by-products. *Food Res Int* 46:488–495. <https://doi.org/10.1016/j.foodres.2011.05.028>
10. dos Santos A, Polidoro ES, Lazzari E et al (2018) Valorization of coffee silverskin industrial waste by pyrolysis: from optimization

- of bio-oil production to chemical characterization by GC × GC/qMS. *J Anal Appl Pyrolysis* 129:43–52. <https://doi.org/10.1016/j.jaap.2017.12.005>
11. Reichembach LH, Guerrero P, de Oliveira Petkowicz CL, de la Caba K (2024) Valorization of pectins from coffee wastes for the development of pectin-chitosan films. *Carbohydr Polym* 334:122057. <https://doi.org/10.1016/j.carbpol.2024.122057>
 12. Laili N, Indrasti NS, Yani M, Djatna T (2024) Coffee waste management using valorization technology: potential development of Eco-Industrial Park in Jember Regency, Indonesia. *EnvironmentAsia* 17:133–147
 13. Kim C-H, Lee S-Y, Park S-J (2024) Valorization of waste coffee grounds into microporous carbon materials for CO₂ adsorption. *Green Chem* 26:1901–1909. <https://doi.org/10.1039/D3GC03557C>
 14. Král E, Rukov JL, Mendes AC (2024) Coffee cherry on the top: disserting valorization of coffee pulp and husk. *Food Eng Rev* 16:146–162. <https://doi.org/10.1007/s12393-023-09352-4>
 15. Duangjai A, Suphrom N, Wungrath J et al (2016) Comparison of antioxidant, antimicrobial activities and chemical profiles of three coffee (*Coffea arabica* L.) pulp aqueous extracts. *Integr Med Res* 5:324–331. <https://doi.org/10.1016/j.imr.2016.09.001>
 16. El-Wakil N, Taha M, Abouzeid R, Dufresne A (2024) Dissolution and regeneration of cellulose from N-methylmorpholine N-oxide and fabrication of nanofibrillated cellulose. *Biomass Convers Biorefin* 14:5399–5410. <https://doi.org/10.1007/s13399-022-02841-2>
 17. Yun T, Tao Y, Li Q et al (2023) Superhydrophobic modification of cellulosic paper-based materials: fabrication, properties, and versatile applications. *Carbohydr Polym* 305:120570. <https://doi.org/10.1016/j.carbpol.2023.120570>
 18. Tanpichai S, Boonmahitthisud A, Soykeabkaew N, Ongthip L (2022) Review of the recent developments in all-cellulose nanocomposites: properties and applications. *Carbohydr Polym* 286:119192. <https://doi.org/10.1016/j.carbpol.2022.119192>
 19. Dong J, Zeng J, Li P et al (2023) Mechanically strong nanopapers based on lignin containing cellulose micro- and nano-hybrid fibrils: lignin content-fibrils morphology-strengthening mechanism. *Carbohydr Polym* 311:120753. <https://doi.org/10.1016/j.carbpol.2023.120753>
 20. Patel R, Trivedi R, Raj M, Raj L (2023) A brief review of polymeric blends based on natural polymers and synthetic thermoplastics polymers. *Chem Pap*. <https://doi.org/10.1007/s11696-023-03139-x>
 21. Madivoli ES, Wanakai SI, Kimani PK et al (2024) Dimethyl amine detection using polydiacetylene functionalized cellulose paper. *ChemistrySelect* 9:1–9. <https://doi.org/10.1002/slct.202304996>
 22. Joyline G, Gachoki KP, Ngure GA et al (2023) High swelling carboxymethyl cellulose synthesized from coconut fibers. *J Natural Fibers* 20:1–14. <https://doi.org/10.1080/15440478.2023.2283549>
 23. Madivoli E (2023) Polysaccharide based hydrogels in drug delivery systems, wound healing, and agriculture. *Chemistry Africa* 6:2281–2295. <https://doi.org/10.1007/s42250-023-00689-1>
 24. Devarajan MM, Kumaraguruparan G, Nagarajan KJ, Vignesh C (2024) Production of hybrid AgNPs - TEMPO-mediated oxidation cellulose composite from jackfruit peduncle agro-waste and its thermal management application in electronic devices. *Int J Biol Macromol* 254:127848. <https://doi.org/10.1016/j.ijbiomac.2023.127848>
 25. Albornoz-Palma G, Ching D, Valerio O et al (2020) Effect of lignin and hemicellulose on the properties of lignocellulose nanofibril suspensions. *Cellulose* 27:10631–10647. <https://doi.org/10.1007/s10570-020-03304-5>
 26. M'barek I, Isik Z, Ozay Y et al (2022) Nanocellulose synthesis from *Tamarix aphylla* and preparation of hybrid nanocellulose composites membranes with investigation of antioxidant and antibacterial effects. *Sep Purif Technol* 292:120815. <https://doi.org/10.1016/j.seppur.2022.120815>
 27. Norrahim MNF, Jenol MA, Nurazzi NM et al (2023) Performance evaluation of nanocellulose-reinforced biopolymer composites. In: *Synthetic and Natural Nanofillers in Polymer Composites*. Elsevier, pp 273–287. <https://doi.org/10.1016/B978-0-443-19053-7.00010-X>
 28. Wang L, Zhu X, Chen X et al (2022) Isolation and characteristics of nanocellulose from hardwood pulp via phytic acid pretreatment. *Ind Crops Prod* 182:114921. <https://doi.org/10.1016/j.indcrop.2022.114921>
 29. Trivedi AK, Gupta MK (2023) An efficient approach to extract nanocrystalline cellulose from sisal fibers: structural, morphological, thermal and antibacterial analysis. *Int J Biol Macromol* 233:123496. <https://doi.org/10.1016/j.ijbiomac.2023.123496>
 30. Sapuan SM, Harussani MM, Ismail AH et al (2024) Development of nanocellulose fiber reinforced starch biopolymer composites: a review. *Phys Sci Rev* 9:1171–1211. <https://doi.org/10.1515/psr-2022-0007>
 31. Mahardika M, Amelia D, Azril SE (2023) Applications of nanocellulose and its composites in bio packaging-based starch. *Mater Today Proc* 74:415–418. <https://doi.org/10.1016/j.matpr.2022.11.138>
 32. Madivoli ES, Kareru PG, Gichuki J, Elbagoury MM (2022) Cellulose nanofibrils and silver nanoparticles enhances the mechanical and antimicrobial properties of polyvinyl alcohol nanocomposite film. *Sci Rep* 12:19005. <https://doi.org/10.1038/s41598-022-23305-7>
 33. Otenda BV, Kareru PG, Madivoli ES et al (2022) Starch-hibiscus-cellulose nanofibrils composite films as a model antimicrobial food packaging material. *J Nat Fibers* 19:12371–12384. <https://doi.org/10.1080/15440478.2022.2058674>
 34. Raghav GR, Nagarajan KJ, Palaninatharaja M et al (2023) Reuse of used paper egg carton boxes as a source to produce hybrid AgNPs- carboxyl nanocellulose through bio-synthesis and its application in active food packaging. *Int J Biol Macromol* 249:126119. <https://doi.org/10.1016/j.ijbiomac.2023.126119>
 35. Rajan STK, Nagarajan KJ, Balasubramani V et al (2023) Investigation of mechanical and thermo-mechanical characteristics of silane-treated cellulose nanofibers from agricultural waste reinforced epoxy adhesive composites. *Int J Adhes Adhes* 126:103492. <https://doi.org/10.1016/j.ijadhadh.2023.103492>
 36. Nagarajan KJ, Ramanujam NR, Sanjay MR et al (2021) A comprehensive review on cellulose nanocrystals and cellulose nanofibers: pretreatment, preparation, and characterization. *Polym Compos* 42:1588–1630. <https://doi.org/10.1002/pc.25929>
 37. James A, Rahman MR, Mohamad Said KA et al (2024) A review of nanocellulose modification and compatibility barrier for various applications. *J Thermoplast Compos Mater* 37:2149–2199. <https://doi.org/10.1177/08927057231205451>
 38. Reis RS, Tienne LGP, de Souza DHS et al (2020) Characterization of coffee parchment and innovative steam explosion treatment to obtain microfibrillated cellulose as potential composite reinforcement. *J Mater Res Technol* 9:9412–9421. <https://doi.org/10.1016/j.jmrt.2020.05.099>
 39. Al Abdallah H, Tannous JH, Abu-Jdayil B (2024) Cellulose and nanocellulose aerogels, their preparation methods, and potential applications: a review. *Cellulose* 31:2001–2029. <https://doi.org/10.1007/s10570-024-05743-w>
 40. Claro FC, Jordão C, de Viveiros BM et al (2020) Low cost membrane of wood nanocellulose obtained by mechanical defibrillation for potential applications as wound dressing. *Cellulose* 27:10765–10779. <https://doi.org/10.1007/s10570-020-03129-2>
 41. Panyamao P, Charumanee S, Ruangsuriya J, Saenjum C (2023) Efficient isolation of cellulosic fibers from coffee parchment via natural acidic deep eutectic solvent pretreatment for nanocellulose production. *ACS Sustain Chem Eng* 11:13962–13973. <https://doi.org/10.1021/acssuschemeng.3c02679>
 42. Henao Rodríguez JE, Escobar Rincón D, Hincapié Rojas DF et al (2023) Effects of hydrolysis and bleaching conditions on

- the efficiency of cellulose microfibrils extraction from coffee parchment through a design of experiments. *Cellulose* 30:10715–10731. <https://doi.org/10.1007/s10570-023-05553-6>
43. Malarat S, Khongpun D, Limtong K et al (2023) Preparation of nanocellulose from coffee pulp and its potential as a polymer reinforcement. *ACS Omega* 8:25122–25133. <https://doi.org/10.1021/acsomega.3c02016>
 44. Campuzano F, Escobar DM, Torres LAM (2023) Simple method for obtaining regenerated cellulose nanoparticles from delignified coffee parchment, and their use in fabricating blended films. *Cellulose* 30:7681–7694. <https://doi.org/10.1007/s10570-023-05368-5>
 45. Demuner IF, Borges Gomes FJ, Coura MR et al (2024) Chemical modification of kraft lignin using black liquor heat treatment. *Nord Pulp Paper Res J*. <https://doi.org/10.1515/npprj-2023-0091>
 46. Coura MR, Demuner AJ, Demuner IF et al (2023) Coffee biomass residue as a raw material for cellulose production and Py-GC/MS analysis. *Waste Biomass Valorization*. <https://doi.org/10.1007/s12649-023-02156-x>
 47. Scandinavian pulp, paper and board testing committee - scan test methods (1993) SCAN-CM 71:09. Stockholm, SWE
 48. Technical association of the pulp and paper - TAPPI standards (2006) Tappi test methods. Atlanta, US
 49. Scott RW (1979) Colorimetric determination of hexuronic acids in plant materials. *Anal Chem* pp 936–941. <https://doi.org/10.1021/ac50043a036>
 50. Segal L, Creely JJ, Martin AE, Conrad CM (1959) An empirical method for estimating the degree of crystallinity of native cellulose using the x-ray diffractometer. *Text Res J* 29:786–794. <https://doi.org/10.1177/004051755902901003>
 51. Ribes DD, Zanatta P, Gatto DA et al (2018) Produção de suspensões nanofibrilares de celulose vegetal por meio de processo combinado – avaliação do gasto energético. *Matéria (Rio de Janeiro)* 23:1–9. <https://doi.org/10.1590/s1517-707620180004.0603>
 52. Wang QQ, Zhu JY, Gleisner R et al (2012) Morphological development of cellulose fibrils of a bleached eucalyptus pulp by mechanical fibrillation. *Cellulose* 19:1631–1643. <https://doi.org/10.1007/s10570-012-9745-x>
 53. Lavoine N, Desloges I, Dufresne A, Bras J (2012) Microfibrillated cellulose – its barrier properties and applications in cellulosic materials: a review. *Carbohydr Polym* 90:735–764. <https://doi.org/10.1016/j.carbpol.2012.05.026>
 54. Vera-Loor A, Rigou P, Marlin N et al (2022) Oxidation treatments to convert paper-grade eucalyptus kraft pulp into microfibrillated cellulose. *Carbohydr Polym* 296:119946. <https://doi.org/10.1016/j.carbpol.2022.119946>
 55. Pääkkö M, Ankerfors M, Kosonen H et al (2007) Enzymatic hydrolysis combined with mechanical shearing and high-pressure homogenization for nanoscale cellulose fibrils and strong gels. *Biomacromol* 8:1934–1941. <https://doi.org/10.1021/bm061215p>
 56. Plackett D, Anturi H, Hedenqvist M et al (2010) Physical properties and morphology of films prepared from microfibrillated cellulose and microfibrillated cellulose in combination with amylopectin. *J Appl Polym Sci* n/a-n/a. <https://doi.org/10.1002/app.32254>
 57. Spence KL, Venditti RA, Habibi Y et al (2010) The effect of chemical composition on microfibrillar cellulose films from wood pulps: mechanical processing and physical properties. *Bioresour Technol* 101:5961–5968. <https://doi.org/10.1016/j.biortech.2010.02.104>
 58. Iwamoto S, Lee S-H, Endo T (2014) Relationship between aspect ratio and suspension viscosity of wood cellulose nanofibers. *Polym J* 46:73–76. <https://doi.org/10.1038/pj.2013.64>
 59. Jiang Y, Liu X, Yang Q et al (2018) Effects of residual lignin on mechanical defibrillation process of cellulosic fiber for producing lignocellulose nanofibrils. *Cellulose* 25:6479–6494. <https://doi.org/10.1007/s10570-018-2042-6>
 60. de Carvalho DM, Moser C, Lindström ME, Sevastyanova O (2019) Impact of the chemical composition of cellulosic materials on the nanofibrillation process and nanopaper properties. *Ind Crops Prod* 127:203–211. <https://doi.org/10.1016/j.indcrop.2018.10.052>
 61. Chen Y, Fan D, Han Y et al (2018) Effect of high residual lignin on the properties of cellulose nanofibrils/films. *Cellulose* 25:6421–6431. <https://doi.org/10.1007/s10570-018-2006-x>
 62. Wen Y, Yuan Z, Liu X et al (2019) Preparation and Characterization of Lignin-Containing Cellulose Nanofibril from Poplar High-Yield Pulp via TEMPO-Mediated Oxidation and Homogenization. *ACS Sustain Chem Eng* 7:6131–6139. <https://doi.org/10.1021/acssuschemeng.8b06355>
 63. Li J, Gellerstedt G (1997) On the structural significance of kappa number measurement. In: International symposium of wood pulping chemical. Montreal, Canadá, pp 56–71
 64. Giudicianni P, Gargiulo V, Alfè M et al (2019) Slow pyrolysis of xylan as pentose model compound for hardwood hemicellulose: a study of the catalytic effect of Na ions. *J Anal Appl Pyrolysis* 137:266–275. <https://doi.org/10.1016/j.jaap.2018.12.004>
 65. Demuner IF, Colodette JL, Gomes FJB, de Oliveira RC (2020) Study of LCNF and CNF from pine and eucalyptus pulps. *Nord Pulp Paper Res J* 35:670–684. <https://doi.org/10.1515/npprj-2019-0075>
 66. Bondam AF, Diolinda da Silveira D, Pozzada dos Santos J, Hoffmann JF (2022) Phenolic compounds from coffee by-products: extraction and application in the food and pharmaceutical industries. *Trends Food Sci Technol* 123:172–186. <https://doi.org/10.1016/j.tifs.2022.03.013>
 67. Zanão M, Colodette JL, Oliveira RC et al (2019) Evaluation of kraft-PS Cooking for eucalypt and pine wood chip mixtures. *J Wood Chem Technol* 39:149–165. <https://doi.org/10.1080/02773813.2018.1533979>
 68. Dias MC, Mendonça MC, Damásio RAP et al (2019) Influence of hemicellulose content of eucalyptus and pinus fibers on the grinding process for obtaining cellulose micro/nanofibrils. *Holzforchung* 73:1035–1046. <https://doi.org/10.1515/hf-2018-0230>
 69. Cangussu LB, Melo JC, Franca AS, Oliveira LS (2021) Chemical characterization of coffee husks, a by-product of coffea arabica production. *Foods* 10:3125. <https://doi.org/10.3390/foods10123125>
 70. Mendoza Martinez CL, Alves Rocha EP, de Oliveira Carneiro AC et al (2019) Characterization of residual biomasses from the coffee production chain and assessment the potential for energy purposes. *Biomass Bioenergy* 120:68–76. <https://doi.org/10.1016/j.biombioe.2018.11.003>
 71. Nunes CA, Lima CF, Barbosa LCA et al (2010) Determination of eucalyptus spp lignin S/G ratio: a comparison between methods. *Bioresour Technol* 101:4056–4061. <https://doi.org/10.1016/j.biortech.2010.01.012>
 72. Pinto PC, Evtuguin DV, Neto CP (2005) Effect of structural features of wood biopolymers on hardwood pulping and bleaching performance. *Ind Eng Chem Res* 44:9777–9784. <https://doi.org/10.1021/ie050760o>
 73. Collins CH, Braga GL, BONATO PS (Coord) (1990) Introdução a métodos cromatográficos. Editora da UNICAMP
 74. Gutiérrez A, Rodríguez IM, del Río JC (2006) Chemical characterization of lignin and lipid fractions in industrial hemp bast fibers used for manufacturing high-quality paper pulps. *J Agric Food Chem* 54:2138–2144. <https://doi.org/10.1021/jf052935a>
 75. Puri S, Sharma S, Kumari A et al (2023) Extraction of lignocellulosic constituents from cow dung: preparation and characterisation of nanocellulose. *Biomass Convers Biorefin* 13:311–320. <https://doi.org/10.1007/s13399-020-01119-9>
 76. Ludeña L, Fasce D, Alvarez VA, Stefani PM (2011) Nanocellulose from rice husk following alkaline treatment to remove silica. *BioRes* 6:1440–1453. <https://doi.org/10.15376/biores.6.2.1440-1453>

77. Littardi P, Rinaldi M, Grimaldi M et al (2020) Effect of addition of green coffee parchment on structural, qualitative and chemical properties of gluten-free bread. *Foods* 10:5. <https://doi.org/10.3390/foods10010005>
78. Ass BAP, Belgacem MN, Frollini E (2006) Mercerized linters cellulose: characterization and acetylation in N, N-dimethylacetamide/lithium chloride. *Carbohydr Polym* 63:19–29. <https://doi.org/10.1016/j.carbpol.2005.06.010>
79. Li J, Wang Z, Wang P et al (2024) Effects of hydrolysis conditions on the morphology of cellulose II nanocrystals (CNC-II) derived from mercerized microcrystalline cellulose. *Int J Biol Macromol* 258:128936. <https://doi.org/10.1016/j.ijbiomac.2023.128936>
80. Raju V, Revathiswaran R, Subramanian KS et al (2023) Isolation and characterization of nanocellulose from selected hardwoods, viz., eucalyptus tereticornis Sm. and Casuarina equisetifolia L., by steam explosion method. *Sci Rep* 13:1199. <https://doi.org/10.1038/s41598-022-26600-5>
81. Oliveira BMRG (2017) Nanostructured films developed from pseudostem of banana and coffee husk. Thesis (PhD in Biomaterials Engineering) – Federal University of Lavras. Lavras, p 145
82. Mahardika M, Abrial H, Kasim A et al (2018) Production of Nanocellulose from Pineapple Leaf Fibers via High-Shear Homogenization and Ultrasonication. *Fibers* 6:28. <https://doi.org/10.3390/fib6020028>
83. Berto GL, Arantes V (2019) Kinetic changes in cellulose properties during defibrillation into microfibrillated cellulose and cellulose nanofibrils by ultra-refining. *Int J Biol Macromol* 127:637–648. <https://doi.org/10.1016/j.ijbiomac.2019.01.169>
84. Asyraf MRM, Ishak MR, Norrrahim MNF et al (2021) Recent advances of thermal properties of sugar palm lignocellulosic fibre reinforced polymer composites. *Int J Biol Macromol* 193:1587–1599. <https://doi.org/10.1016/j.ijbiomac.2021.10.221>
85. Mohamad Haafiz MK, Eichhorn SJ, Hassan A, Jawaid M (2013) Isolation and characterization of microcrystalline cellulose from oil palm biomass residue. *Carbohydr Polym* 93:628–634. <https://doi.org/10.1016/j.carbpol.2013.01.035>
86. Mandal A, Chakrabarty D (2011) Isolation of nanocellulose from waste sugarcane bagasse (SCB) and its characterization. *Carbohydr Polym* 86:1291–1299. <https://doi.org/10.1016/j.carbpol.2011.06.030>
87. Kim H-J, Roy S, Rhim J-W (2021) Effects of various types of cellulose nanofibers on the physical properties of the CNF-based films. *J Environ Chem Eng* 9:106043. <https://doi.org/10.1016/j.jece.2021.106043>
88. Mhlongo JT, Nuapia Y, Motsa MM et al (2022) Green chemistry approaches for extraction of cellulose nanofibers (CNFs): a comparison of mineral and organic acids. *Mater Today Proc* 62:S57–S62. <https://doi.org/10.1016/j.matpr.2022.02.088>
89. Sharma A, Mandal T, Goswami S (2021) Dispersibility and stability studies of cellulose nanofibers: implications for nanocomposite preparation. *J Polym Environ* 29:1516–1525. <https://doi.org/10.1007/s10924-020-01974-7>
90. Xu S, Huo D, Wang K et al (2021) Facile preparation of cellulose nanofibrils (CNFs) with a high yield and excellent dispersibility via succinic acid hydrolysis and NaClO₂ oxidation. *Carbohydr Polym* 266:118118. <https://doi.org/10.1016/j.carbpol.2021.118118>
91. Damasio RAP (2015) Characterization and nanoscale applications of nanofibrillated cellulose (NFC) and cellulose nanocrystals (CNC). Dissertation (Master's in Forestry Science) – Federal University of Viçosa. Viçosa, p 91
92. Chen JH, Liu JG, Su YQ, Xu ZH, Li MC, Ying RF, Wu JQ (2019) Preparation and properties of microfibrillated cellulose with different carboxyethyl content. *Carbohydr Polym* 206:616–624. <https://doi.org/10.1016/j.carbpol.2018.11.024>
93. Hu L, Xu W, Gustafsson J et al (2022) Water-soluble polysaccharides promoting production of redispersible nanocellulose. *Carbohydr Polym* 297:119976. <https://doi.org/10.1016/j.carbpol.2022.119976>
94. Xu Q, Gao Y, Qin M et al (2013) Nanocrystalline cellulose from aspen kraft pulp and its application in deinked pulp. *Int J Biol Macromol* 60:241–247. <https://doi.org/10.1016/j.ijbiomac.2013.05.038>
95. Winuprasith T, Suphantharika M (2013) Microfibrillated cellulose from mangosteen (*Garcinia mangostana* L.) rind: preparation, characterization, and evaluation as an emulsion stabilizer. *Food Hydrocoll* 32:383–394. <https://doi.org/10.1016/j.foodhyd.2013.01.023>
96. Cheng Q, Wang J, Mcneel JF, Jacobson PM (2010) Water retention value measurements of cellulosic materials using a centrifuge technique. *BioRes* 5:1945–1954. <https://doi.org/10.15376/biores.5.3.1945-1954>

Publisher's Note Springer Nature remains neutral with regard to jurisdictional claims in published maps and institutional affiliations.

Springer Nature or its licensor (e.g. a society or other partner) holds exclusive rights to this article under a publishing agreement with the author(s) or other rightsholder(s); author self-archiving of the accepted manuscript version of this article is solely governed by the terms of such publishing agreement and applicable law.